ELSEVIER

Journal of Power Sources 114 (2003) 285–291

JOURNAL OF POWER SOURCES

www.elsevier.com/locate/jpowsour

Identity and thermodynamics of lithium intercalated in graphite

Hsiang-Hwan Lee, Chi-Chao Wan*, Yung-Yun Wang

Department of Chemical Engineering, National Tsing-Hwa University, Hsinchu 300, Taiwan

Received 30 July 2002; accepted 26 October 2002

Abstract

The intercalation of Li into layer-structure materials is closely compared with the features of underpotential deposition (UPD). Based on the initiation potential adsorption behaviour, cyclic voltammetric and impedance response of Li_XC_6, it is proposed that Li intercalation can be considered to be a special type of UPD with the substrate being a layered structure. The thermodynamic behaviour of Li intercalation in graphite can be interpreted in terms of an adsorption isotherm and an inverse derivative curve. The thermodynamic equation of the adsorption isotherm, including the long-range interaction energy between Li atoms, has been used and a close match has been found with the result in the final two phase transitions of cell discharge.

Keywords: Adsorption isotherm; Intercalation; Underpotential deposition; Lithium-ion batteries

1. Introduction

Graphite carbon is the most commonly used material for the negative electrode (anode) of Li-ion batteries. This is because of its low charging voltage and wide range of lithium insertion [1]. Its basic building block is a planar sheet of carbon atoms arranged in a honeycomb structure. These carbon layers are stacked in a registered order. When Li atoms intercalate into graphite, Li can reside in the centre of the van der Waals gap between adjacent carbon layers, and then position itself in the centre of the carbon hexagons of the stacked carbon layers. Every Li atom is located on a hexagonal superlattice with a lattice constant $\sqrt{3}$ times the graphite *a*-axis so that no pairs of Li atoms occupy the nearest neighbouring sites. In such a structure, there is exactly one Li for every six carbon atoms (LiC_6) with a specific charge of 372 mAh g^{-1} [1–3].

Numerous studies on Li intercalation in various carbon materials have been published. These have examined the intercalation mechanism, intercalated Li properties, electrochemical performance, and so on. The true identity of intercalated Li in the carbon electrodes has not, however, been ascertained. Early research claimed that the intercalated Li in graphite was in ionic state by theoretical calculation [4,5], X-ray photoelectron spectroscopy (XPS) [6], and ^{7}Li nuclear magnetic resonance (NMR) [7]. Hence, Li in LiC_6 is written as the reaction for Li ion in many reports. Based on electrochemical theory, however, it seems logical to assume that the Li ions in electrolytes should accept electrons from the outer electric circuit and then be reduced to elemental Li, just as would occur on a metal electrode. The only difference is that the Li atoms are adsorbed in the matrix rather than being deposited in a continuous metallic film on a metal electrode. In fact, the reduction potentials for the two systems are basically the same since the reactions should be the same, i.e. charge transfer between lithium ions and the lithium element. The ionic character of Li in LiC_6 may result from some interactions between Li atoms or between Li atoms and the carbon matrix, which results in partial redistribution of charge. Thus, positively charged Li and covalent Li may be observed simultaneously. This view has also been supported by Hightower et al. [8] by using electron energy-loss spectrometry (EELS) and Song et al. [9] by using the effective atomic charge of Li. The identity of Li after intercalation is therefore not fully established if the electrode is a layered-structure carbon matrix.

In fact, if the intercalated Li is still in an ionic state and not reduced after charging, this would mean that the oxidation reaction occurring on the positive electrode is not balanced by a reduction reaction on the negative electrode, which is contrary to electrochemical theory. In addition, LiC_6 can even be obtained by contacting gaseous or liquid lithium to graphite at specific temperature and pressure [3]. Under these circumstances, the Li must be in elemental form after intercalation. Other evidence comes from the fact that LiC_6

* Corresponding author.
E-mail address: ccwan@mx.nthu.edu.tw (C.-C. Wan).

0378-7753/03/$ – see front matter
doi:10.1016/S0378-7753(02)00606-7

has almost the same activity to water as Li metal when in contact with water. If LiC_6 is immersed in water, smoke and gas evolve immediately. This is very difficult to explain if the Li in LiC_6 is in ionic state. Thus, this study explores the identity of Li when intercalated in graphite after charging.

2. Experimental

The preparation of liquid electrolyte, polymer membrane electrolyte, and cell assembly was performed in an argon-filled glove box (Model MB 150-M, Mbraun) or dry room within which the moisture content of the atmosphere was controlled to under 2 ppm. Artificial graphite material (TIMCAL AG, Sins, Switzerland, code TIMREX SGF44) was used as a test carbon. SFG44 graphite electrodes were prepared by spreading a slurry, which contained graphite powder and PVDF/HFP copolymer (Kynar FLEX® 2801, Elf Atochem North America Inc.) dissolved in acetonitrile (TEDIA, USA), on to a copper current-collector. The graphite loading on the current-collector was 10 mg cm^{-2}. Electrodes were then punched out in the form of 12 mm diameter disks for cell assembly. Coin cells (type 2030) were assembled with Li foil as the counter electrode. A mixed electrolyte which contained equal molar amounts of ethylene carbonate (EC, Merck) and γ-butyrolactone (γ-BL, Merck) with 1 M $LiPF_6$ (Hashimoto, Japan) was used in all tests.

Cyclic voltammetry, hole-potential tests, and ac impedance tests were all operated by means of AUTOLAB (Eco Chemie, Holland) with general purpose electrochemical system (GPES) and frequency response analyzer (FRA) program software. Cyclic voltammograms were measured at a 5 μV s^{-1} scan rate. Cell impedance was measured (OCV is 0.05 V versus Li/Li^+) by applying an ac bias of 10 mV amplitude with a frequency from 50 kHz to 0.01 Hz. In the continuously changing potential test, a constant current 0.1 mA cm^{-2} was provided from a MACCOR series 4000 tester.

3. Results and discussion

3.1. Comparison between UPD and Li intercalation into graphite

Intercalation compounds with a layer structure, e.g. TiS_2, MoS_2, MnO_2, CoO_2, graphite and carbonaceous materials, are widely used in Li-ion batteries. Since intercalation reactions are intrinsically simple and reversible, they are ideal for battery cycling. During the discharge and the charge processes, Li ions (known as 'guests') intercalate into these layer-structure materials (known as 'hosts') and occupy sites within the framework. It is interesting to note that the geometry of the host does not change and the Li atoms can enter or leave the host lattice reversibly, which results in a varying and non-stoichiometric Li concentration. Thus, Li intercalation systems provide some interesting points from the viewpoint of the statistical thermodynamics of the lattice occupancy in a solid phase [10,11]. Conway [12] was the first to note that Li intercalation in transition metal oxides or chalcogenides is closely analogous to two-dimensional underpotential deposition (UPD), and termed these intercalation systems 'quasi-two-dimensional UPD'. By this notion, Li intercalation and metal UPD are two similar, but different, processes. Nevertheless, the reason for the difference in the processes has not been reported in the literature.

UPD is a process in which metal atoms are deposited on to a foreign substrate at a potential positive to its reversible potential. Adžic [13] suggested that, in UPD, the deposition of metal atoms forms only a monolayer rather than a bulk metal film as in conventional electrodeposition. Generally speaking, UPD functions as a form of chemical adsorption so that it can be illustrated in terms of thermodynamic adsorption isotherms [14]. Interestingly, intercalation of Li in layer-structure materials has similar properties, as pointed out by Conway [12] for a $LiTS_2$ substrate. Further elaboration of these similarities is reported here and is based on data obtained from graphite anodes.

3.1.1. Potential

One of the fundamental definitions of UPD is that its potential of deposition occurs more positive than the reversible potential. This means that the attractive force between deposited atoms and substrate in UPD is larger than that in conventional metal deposition. This also holds true for intercalation of Li in graphite. Cyclic voltammetry is a powerful analytical tool for obtaining the real potential of

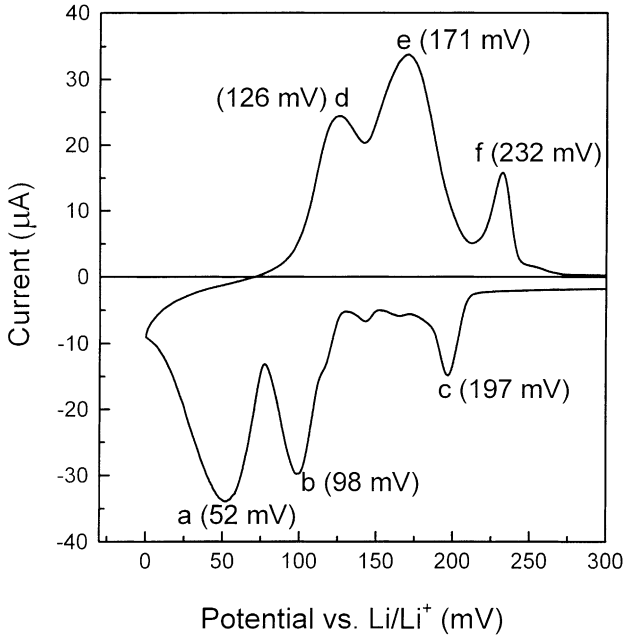

Fig. 1. Cyclic voltammogram for Li intercalation in SFG44 graphite. Scan rate is 5 μV s^{-1}. The graphite electrode is a very thin layer coating on copper and its area is 0.25 cm^2, which is quarter of that of Li counter electrode. Electrolyte is 1 M $LiPF_6$ in EC + γ-BL (1:1).

intercalation. A 5 mm × 5 mm copper foil was dipped into a graphite slurry to produce a special working electrode which was thinly coated with graphite. A lithium metal electrode (12 mm diameter) was used as the counter electrode. As shown Fig. 1, three sets of well-defined peaks appear in the voltammogram and are associated with phase transfer between the Li–graphite intercalation stages, which has also been reported earlier [15]. Owing to the large particle size (∼44 μm) and limited instrument resolution, these peaks appear both wide and smooth. The cathodic peaks a, b, c at 52, 98, 197 mV versus Li/Li^+ correspond to stage-wise Li intercalation. The anodic peaks d, e, f at 126, 171, 232 mV versus Li/Li^+ correspond to Li de-intercalation. Thus, the potential of Li intercalation in graphite starts at about 200 mV more positive to the reversible potential of lithium metal deposition and dissolution. This property matches exactly the definition of UPD.

Furthermore, the peaks in Fig. 1 represent different stages of the transition [12,15]. Such phenomenon is again closely analogous to a typical two-dimensional UPD process which involves multiple-state adsorption in monolayers [14,16]. Multiple-state adsorption indicates that the deposited atoms have different lattice structures. The peaks in the cyclic voltammogram display the phase transfer between various lattice structures in UPD.

3.1.2. Potential curve

Another feature of UPD is a continuously changing potential with increasing adsorption, which is represented by the fraction of surface occupancy, θ, ranging from 0 to 1 [13,14]. The electric potential of Li intercalation in layered-hosts displays a continuous variation with the content of intercalated Li. This is unlike a metal deposition and dissolution system which exhibits a relatively flat potential profile inside the electrode. Thompson [17] has reported the characteristics of the discharge curve of Li intercalation in Li_XTiS_2. This is an almost ideal example of a continuous, sigmoid discharge curve, which closely resembles the theoretical Langmuir-type isotherm of UPD [11,16,17]. Nevertheless, intercalation of Li into a graphite system displays a more complicated change in potential, as shown in Fig. 2. It was pointed out earlier that the continuously varying electrode potential corresponds to a continuous change in the chemical potential of Li in graphite which, in turn, is due to formation of a compound with a varying Li:C ratio, i.e.

$$X\mathrm{Li} + \mathrm{C_6} \rightarrow \mathrm{Li}_X\mathrm{C_6} \quad (0 < X \leq 1.0\,\text{intercalation}) \tag{1}$$

There is another stoichiometric chemical reaction, as follows:

$$\mathrm{Li} + \mathrm{C_6} \rightarrow \mathrm{LiC_6} \quad (\text{chemical reaction}) \tag{2}$$

According to Eq. (2) C_6 and LiC_6 behave as two pure phases in equilibrium, so that there should be a constant potential value. The intercalation reaction does not, however, obey this rule and its electrode potential changes as X changes, which is exactly the way in which UPD behaves (the potential changes with surface occupancy, θ).

Three clear potential plateaux are shown in Fig. 2 and correspond to a regular multi-stage discharge process. Previous studies [1,3] have also demonstrated that intercalation of Li in graphite proceeds over several regions of continuously declining potential with sharp discontinuities indicative of phase transitions. Earlier workers defined these phase transitions as stage transfers [1–3,15,18]. The first phase transition is at around $X = 0.08$ and corresponds to a high-order stage transfer. The succeeding transitions are at around $X = 0.26$ and 0.55, and correspond to stage III → stage II, stage II → stage I, respectively. These three major plateaux

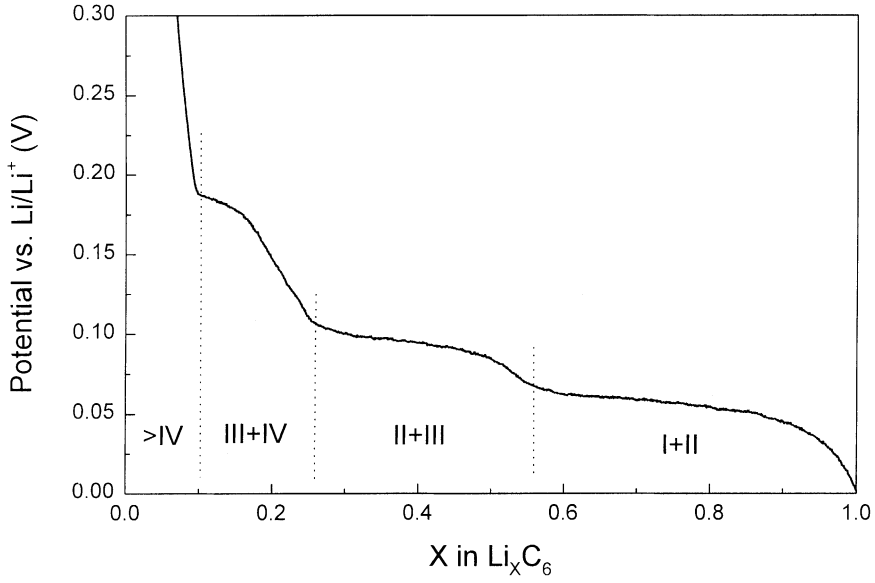

Fig. 2. Continuous decline of electrode potential of Lilgraphite intercalate with varying extent of Li incorporation. The Lilgraphite coin cell is discharged at a constant current of 0.1 mA cm^{-2}. The electrolyte is 1 M $LiPF_6$ in EC + γ-BL (1:1).

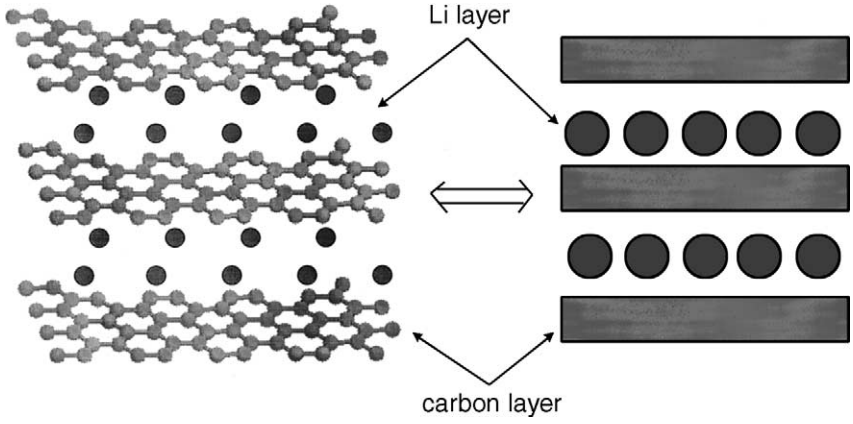

Fig. 3. Structure of GIC with Li. The diagram is drawn according to TEM images and descriptions in [1–3,18].

are also consistent with the peaks in the cyclic voltammogram shown in Fig. 1.

3.1.3. Arrayed structure of deposited atoms

The third major feature of UPD is that the adsorbed metal atoms form only a monolayer [13,14]. The graphite structure is composed of two-dimensional planar layers. When Li atoms intercalate into graphite, Li can reside in the centre of the gap between adjacent carbon layers, namely, the van der Waals gap. Due to the size limitation of the gap, Li atoms in LiC_6 are distributed in a 'single' plane and the stacking order of the lithium inter-layers is αα (a Li–C_6–Li–C_6–Li chain exists along the *c*-axis of graphite [1–3,11,18]), as shown in Fig. 3.

Previous studies [2,18] indicate that many types of atoms or molecular layers can intercalate into graphite to form so-called graphite intercalation compounds (GICs). All GICs have layered structures and special staging phenomena. Dresselhaus and Dresselhaus [2] employed HRTEM to show that the layered structure of the intercalated species forms a monolayer in the same manner as adsorbates of UPD. Intercalation actually proceeds in a three-dimensional solid, but it can be considered to be a quasi-two-dimensional process which takes place between layers of the host structure.

3.1.4. Adsorption features impedance spectroscopy

A three-electrode, ac impedance diagram of a graphite working electrode in a Li|C half cell is presented in Fig. 4. There are two capacitive loops and an inductive loop from high to low frequency. Generally speaking, the left capacitive loop at high frequency results mainly from the passivated layer on the graphite surface that is formed after electrochemical reaction [15]. The right capacitive loop at middle frequency represents charge transfer. The presence of an inductive loop at low frequency is interesting; it usually

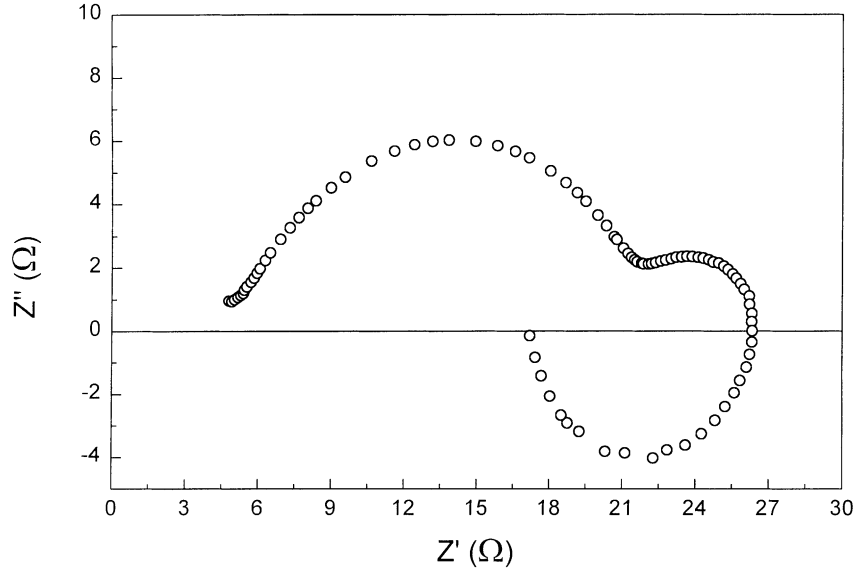

Fig. 4. Three-electrode ac impedance of intercalated graphite working electrode. Open-circuit voltage is 0.05 mV. Counter and reference electrodes are both Li metal. Electrolyte is 1 M $LiPF_6$ in EC + γ-BL (1:1).

exists under conditions of rough electrodes or electrosorption [19]. The same inductive loop was also observed by Nagasubramanian [20]. Hence, it is concluded that this inductive loop corresponds to the Faradic adsorption of Li atoms on the carbon surface during intercalation, as reported by Takasu et al. [21], i.e.

$$-C- + Li^+ + e^- \rightarrow -C-Li_{ad} \quad (3)$$

This is again consistent with the characteristic monolayer adsorption of UPD.

3.1.5. Competition of Li intercalation and bulk Li metal deposition

According to the discussion above, the potential of Li intercalation in graphite is more positive to the reversible potential of lithium metal deposition and dissolution. In other words, the attractive force between deposited Li atoms and graphite is larger than that in conventional Li metal deposition. It also means the Li metal deposition has a higher energy barrier than the intercalation of Li into graphite. To confirm this, potential-hold experiments were performed (see Fig. 5). The potential excitation is shown in Fig. 5a. The cell potential is firstly stepped to a specific voltage, *V*, and then held at this value for a period, *t*. The cathodic current is conserved and indicates either intercalation, or possibly bulk Li metal deposition. The cells are slowly swept from this voltage to 2.0 V at a scan rate of 1 mV s^{-1} to observe the corresponding oxidizing current. The results, shown in Fig. 5b, clearly illustrate the priority of intercalation over bulk deposition of Li. When the holding potential is 0.05, 0, −0.1 and −0.2 versus Li/Li^+, a smooth negative current curve appears and corresponds to continuous intercalation of Li into graphite. Oxidation peaks also appear in the reverse positive current region. When the holding potential is lowered to −0.3 V versus Li/Li^+, however, one additional cathodic and two anodic current peaks appear. Since this voltage (−0.3 V) is sufficiently negative to initiate Li metal deposition, the additional cathodic peak can be assigned to that process. The two anodic peaks demonstrate that there are two reversible reactions. Comparing the voltammograms in Fig. 5b, the electrode shows insufficient bulk Li deposition so that only the intercalation reaction is observed. Evidently, bulk Li phase forms with greater difficulty, e.g. it appears at a potential more negative than the intercalation of Li. This again is consistent with the potential features of UPD. In UPD, bulk metal deposition also starts if the deposition potential is controlled at value much more negative than the UPD potential.

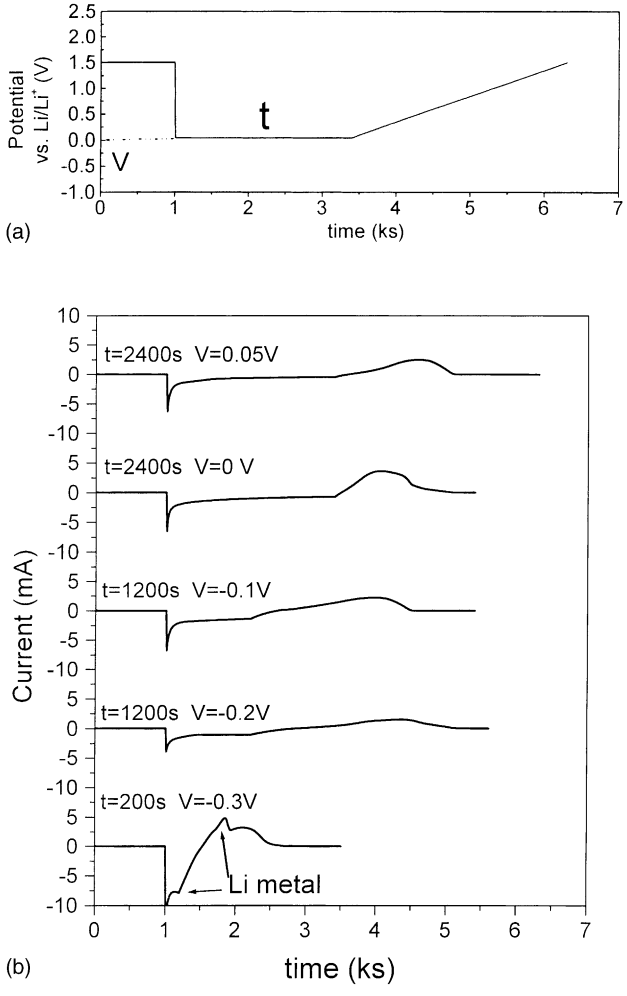

Fig. 5. Potential-hold experiments of LilC half cells. (a) Potential excitation. Potential first stepped at a specific voltage *V* (vs. Li/Li^+) for a period *t*, and then swept at a 1 mV s^{-1} scan rate. (b) Responding current at various *V* and *t* listed in each panel. Electrolyte is 1 M $LiPF_6$ in EC + γ-BL (1:1).

3.2. Thermodynamics of Li intercalation in graphite

If intercalation of Li in graphite can be considered a special UPD process, it should satisfy the thermodynamic theory that describes the adsorption of metal atoms in UPD. In this respect, Conway [12] derived a theoretical representation of intercalation of Li in terms of an adsorption isotherm. Levi and Aurbach [22] recently presented an excellent review of the thermodynamic and kinetic characteristics of the intercalation of Li. Although these workers proposed that the potential profile of intercalation is different from the general adsorption case with a double layer, 'intercalation isotherms' were still derived from metal-type potential distribution, the Frumkin isotherm, and pseudocapacitance, all of which are usually used for the UPD process. Many investigators [11,17,23] have conducted detailed research on Li adsorption for its intercalation into Li_XTiS_2.

In this section, the thermodynamic properties of Li intercalation into graphite are evaluated. First, a lattice gas model is adopted [10,11,22], namely, it is assumed that the intercalated atoms are located at specific sites in the host lattice and that the motion of the intercalated atoms from site to site can be neglected. The experimental results presented here can also be interpreted in terms of this model.

Since *X* is a measure of the charge passed upon intercalation, $\Delta X/\Delta E$ is a quantity which is proportional to the differential intercalation capacity analogous to the adsorption

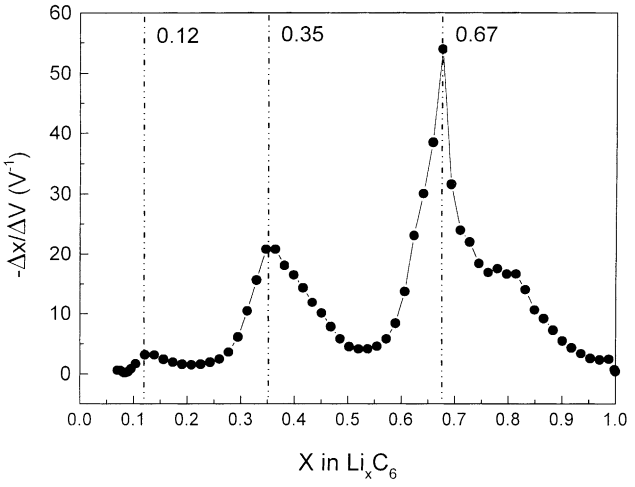

Fig. 6. Experimental inverse differential plot, $\Delta X/\Delta E$, vs. X of Li intercalation in SFG44. Original data is from Fig. 2.

pseudocapacitance of UPD. Hence, the inverse derivative $\Delta X/\Delta E$ of Li intercalation in graphite can be obtained from Fig. 2; it is shown in Fig. 6. The three peaks represent lattice gas phase transitions, which correspond to the plateaux in Fig. 2. This suggests that the Li-rich and Li-poor phases co-exist in this region [24]. Several orders of the phase transition of the intercalation of Li into graphite renders the data presented in Fig. 6 more complicated than that of other intercalation systems. Between the above peaks, there are minima in $-\Delta X/\Delta E$. According to Berlinsky et al. [23], these minima are commensurate phases which are gradually filled with Li atoms. These commensurate phases, which are also a general feature of the lattices gas model, relate to pure and single phases, such as LiC_{12} or LiC_6 [25].

Among the theoretical adsorption models, the simplest is the Langmuir-type isotherm, which assumes random occupancy of the lattice with no interaction. In a real system, the energy of an intercalated atom on a particular site must change in the presence of other atoms. This can be regarded as an interaction between the atoms. Understandably, the Langmuir isotherm exhibits significant deviation from actual data due to this interaction. To modify the Langmuir isotherm, McKinnon [10] and McKinnon and Haering [11] introduced the long-range interaction energy, γU, and then derived a mean field theory based on statistical thermodynamics, i.e.

$$E = \frac{1}{F}\left[E_P^0 + \gamma UX + RT\ln\left(\frac{1-X}{X}\right)\right] \quad (4)$$

where E is the potential of adsorbates, which is a function of the site's occupancy fraction X, R is the gas constant, T the absolute temperature, F the Faraday constant, γ the number of sites that an atom can interact with other atoms that possess an interaction energy U, E_P^0 is the energy of an atom on a specific site.

An attempt was made to fit the Li_XC_6 system in terms of Eq. (4). It is difficult, however, to obtain a good match over the total range of intercalation. This is because the various phase transitions, which inevitably exist in Li_XC_6 and other Li intercalation systems, cannot be fully covered by these methods [12,22,24]. To evaluate the individual stages based on the model represented by Eq. (4), it is assumed that γU, E_P^0 are the factors related to geometry, which change with different stages. A similar approach has also been suggested by Yamaki et al. [26], who used intercalation pressure as the stage factor. By contrast, McKinnon and Haering [11] used site energy E_P^0. An attempt has been made to fit the stages I + II plateaux in terms of Eq. (4), as shown in Fig. 7. The simulated results are in good agreement with the experimental data with $\gamma U = 3.4RT/F$, $E_P^0 = 0.5RT/F$. Apparently, this means that the major

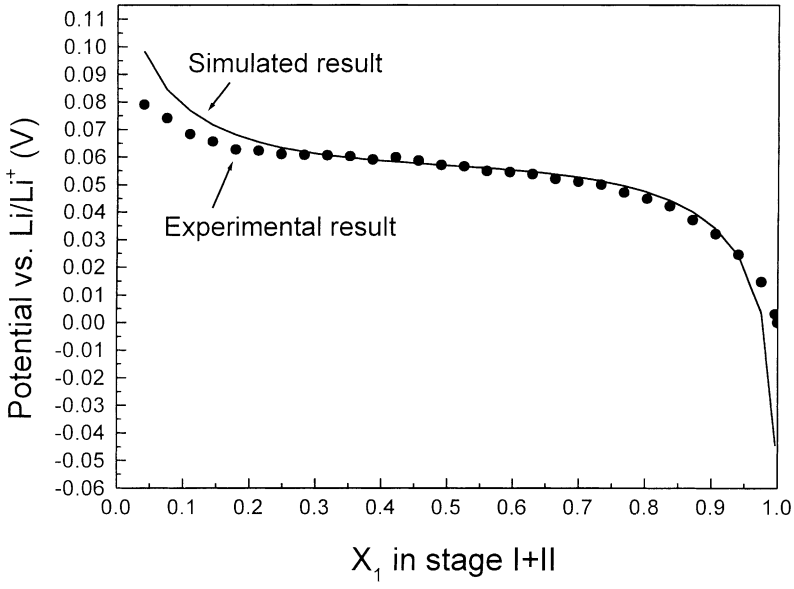

Fig. 7. Simulated and experimental curve of isotherm of Li intercalation in a graphite anode during stages I and II.

factors in stages I + II are the long-range interaction energy between Li atoms and the specific site energy.

Other plateaux have more complicated profiles and it is difficult to obtain a perfect fit with Eq. (4). Strictly speaking, intercalation is a complex phenomenon that involves many steps. The energies involved include the separation energy required to open the van der Waals gap, the elastic energy which results from deformation of the carbon layers, and the different potential energies which Li atoms occupy at different lattice sites. Yamaki et al. [26], for instance, have derived an equation that takes into consideration the intercalation pressure and graphite crystallites. Nevertheless, this equation does not include all the factors and cannot totally match the experimental data. Still, such equations assist the understanding of the thermodynamic behaviour of Li intercalation in graphite.

4. Conclusion

Based on experimental characteristics, which include the potential response and the impedance of Li_XC_6, it is proposed that Li intercalation is not merely analogous to UPD. Rather, it is a special type of UPD with the substrate being a layered structure. The thermodynamic behaviour of Li intercalation in graphite can also be described by an adsorption isotherm and an inverse derivative curve. Multi-peaks shown in the inverse derivative correspond to the pseudocapacitance of adsorption and the co-existence of phases. In addition, a thermodynamic equation relating to the adsorption isotherm can match closely the Li intercalation in the final two phase transitions (stages I and II) during cell discharge.

References

[1] J.R. Dahn, A.K. Sleigh, H. Shi, B.M. Way, W.J. Weydanz, J.N. Reimers, Q. Zhong, U.V. Sacken, in: G. Pistoia (Ed.), Lithium Batteries: New Materials, Developments and Perspectives, Elsevier, Amsterdam, 1994, p. 1.
[2] M. Dresselhaus, G. Dresselhaus, Adv. Phys. 30 (1980) 139.
[3] K. Kinoshita, in: T. Osaka, M. Datta (Eds.), Energy Storage Systems for Electronics, Gordon and Breach, Amsterdam, 2000, p. 193.
[4] N.A.W. Holzwarth, S.G. Louie, S. Rabii, Phys. Rev. B 28 (1983) 1013.
[5] N.A.W. Holzwarth, S.G. Louie, S. Rabii, Phys. Rev. B 30 (1984) 2219.
[6] H. Momose, H. Honbo, S. Takeuchi, K. Nishimura, T. Horiba, Y. Muranaka, Y. Kozono, H. Miyadera, J. Power Sources 68 (1997) 208.
[7] K. Tatsumi, T. Akai, T. Imamura, K. Zaghib, N. Iwashita, S. Higuchi, Y. Sawada, J. Electrochem. Soc. 143 (1996) 1923.
[8] A. Hightower, C.C. Ahn, B. Fultz, Appl. Phys. Lett. 77 (2000) 238.
[9] M.K. Song, S.D. Hong, K.T. No, J. Electrochem. Soc. 148 (2001) A1159.
[10] W.R. McKinnon, in: P.G. Bruce (Ed.), Solid State Electrochemistry, Cambridge University, New York, 1995, p. 163.
[11] W.R. McKinnon, R.R. Haering, in: R.E. White, J.O'M. Bockris, B.E. Conway (Eds.), Modern Aspects of Electrochemistry, vol. 15, Plenum Press, New York, 1983, p. 235.
[12] B.E. Conway, Electrochim. Acta 38 (1993) 1249.
[13] R.R. Adžic, in: H. Gerischer (Ed.), Advances in Electrochemistry and Electrochemical Engineering, vol. 13, Wiley/Interscience, New York, 1984, p. 159.
[14] E. Gileadi, Electrode Kinetics for Chemists, Chemical Engineers, and Materials Scientists, VCH, New York, 1993, p. 261.
[15] B. Markocsky, M.D. Levi, D. Aurbach, Electrochim. Acta 43 (1998) 2287.
[16] B.E. Conway, H.A. Kozlowska, Acc. Chem. Res. 14 (1981) 49.
[17] A.H. Thompson, J. Electrochem. Soc. 126 (1979) 608.
[18] D.M. Hwang, in: H. Zabel, S.A. Solin (Eds.), Graphite Intercalation Compounds. I. Structure and Dynamics, Springer, Germany, 1990, p. 253.
[19] N.A. Hampson, S.A.G.R. Karunathilaka, R. Leek, J. Appl. Electrochem. 10 (1980) 3.
[20] G. Nagasubramanian, J. Power Sources 87 (2000) 226.
[21] R. Takasu, K. Sekine, T. Takamura, J. Power Sources 81–82 (1999) 224.
[22] M.D. Levi, D. Aurbach, Electrochim. Acta 45 (1999) 167.
[23] A.J. Berlinsky, W.G. Unruh, W.R. McKinnon, R.R. Haering, Solid State Commun. 31 (1979) 135.
[24] V.I. Kalikmanov, M.V. Koudriachova, S.W. de Leeuw, Solid State Ionics 136–137 (2000) 1373.
[25] M.D. Levi, E.A. Levi, D. Aurbach, J. Electroanal. Chem. 421 (1997) 89.
[26] J. Yamaki, M. Egashira, S. Okada, J. Electrochem. Soc. 147 (2000) 460.